nature genetics

Abnormal skin, limb and craniofacial morphogenesis in mice deficient for interferon regulatory factor 6 (*Irf6*)

Christopher R Ingraham[1], Akira Kinoshita[1], Shinji Kondo[2], Baoli Yang[3], Samin Sajan[4], Kurt J Trout[1], Margaret I Malik[1], Martine Dunnwald[5], Stephen L Goudy[6], Michael Lovett[4], Jeffrey C Murray[1] & Brian C Schutte[1]

Transcription factor paralogs may share a common role in staged or overlapping expression in specific tissues, as in the Hox family. In other cases, family members have distinct roles in a range of embryologic, differentiation or response pathways (as in the Tbx and Pax families). For the interferon regulatory factor (IRF) family of transcription factors, mice deficient in *Irf1*, *Irf2*, *Irf3*, *Irf4*, *Irf5*, *Irf7*, *Irf8* or *Irf9* have defects in the immune response but show no embryologic abnormalities[1–7]. Mice deficient for *Irf6* have not been reported, but in humans, mutations in *IRF6* cause two mendelian orofacial clefting syndromes[8–10], and genetic variation in *IRF6* confers risk for isolated cleft lip and palate[11–15]. Here we report that mice deficient for *Irf6* have abnormal skin, limb and craniofacial development. Histological and gene expression analyses indicate that the primary defect is in keratinocyte differentiation and proliferation. This study describes a new role for an IRF family member in epidermal development.

To define the role of *Irf6 in vivo*, we generated mice deficient for *Irf6*. We identified an embryonic stem cell line carrying a gene trap allele for *Irf6* in the Omnibank database (OST398253)[16]. Sequence analysis showed that the gene trap vector inserted into intron 1 of *Irf6*, 36 bp from the splice donor site (**Fig. 1a**). We detected the *Irf6* gene trap allele ($Irf6^{gt1}$) by PCR (**Fig. 1b**) and DNA blot analysis (data not shown). We mated mice heterozygous for the gene trap allele ($Irf6^{gt1/+}$), and 18% (34 of 192) of the embryos showed abnormal external morphology (**Fig. 1c,d**). Genotyping demonstrated that all abnormal mice were homozygous for the gene trap allele ($Irf6^{gt1/gt1}$), and their frequency was not significantly different from mendelian ratios ($P = 0.06$). Expression analysis showed Irf6 protein in skin and oral epithelium from E17.5 wild-type embryos, as previously shown[17,18] but reduced expression in skin from heterozygous embryos and no detectable expression in skin from $Irf6^{gt1/gt1}$ embryos (**Fig. 1e**), demonstrating that the gene trap is a null allele for *Irf6*.

Initial analysis did not identify any obvious differences between wild-type and heterozygous E17.5 embryos. However, homozygous $Irf6^{gt1/gt1}$ (null) embryos had taut, shiny skin, lacked external ears and had snouts and jaws shorter and more rounded than their wild-type littermates (**Fig. 1c,d**). The null embryos also had short forelimbs that lacked visible digits and a single caudal projection that lacked visible hindlimbs and tail.

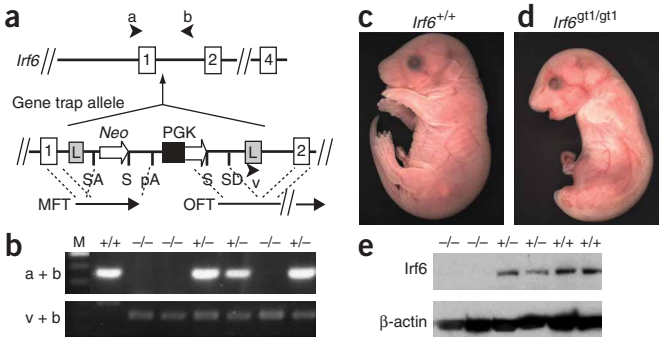

Figure 1 Genotypic and phenotypic analysis of mice deficient for *Irf6*. (**a**) *Irf6* gene trap allele ($Irf6^{gt1}$). The gene trap vector (VICTR48) inserted 36 bp from the splice donor site of intron 1 and contains flanking long terminal repeats (L), a splice acceptor (SA) and donor (SD) sites, the ORF for neomycin (*Neo*), stop codons (S), polyadenylation site (pA), the phosphoglycerate kinase (PGK) promoter, marker fusion transcript (MFT) and OmniBank sequence tag (OST) fusion transcript (OFT). (**b**) Genotypic analysis by PCR of genomic DNA derived from E17.5 embryos using primers a and b to detect wild-type (+) and using primers v and b to detect mutant (–) alleles. (**c**) Gross appearance of wild-type E17.5 embryos. (**d**) E17.5 embryo that is homozygous for gene trap allele ($Irf6^{gt1/gt1}$). (**e**) Protein blot analysis of protein extracts obtained from E17.5 skin from mice with the indicated genotype. Blots were probed with antibodies directed against the indicated protein.

[1]Department of Pediatrics, University of Iowa, Iowa City, Iowa 52242, USA. [2]Division of Functional Genomics, Center for Frontier Life Sciences, Nagasaki University, Nagasaki, Japan. [3]Department of Obstetrics and Gynecology, University of Iowa, Iowa City, Iowa 52242, USA. [4]Department of Genetics, Washington University School of Medicine, St. Louis, Missouri 63110, USA. [5]Department of Dermatology, University of Iowa, Iowa City, Iowa 52242, USA. [6]Department of Otolaryngology, Vanderbilt University, Nashville, Tennessee 37232, USA. Correspondence should be addressed to B.C.S. (brian-schutte@uiowa.edu).

Received 4 August; accepted 12 September; published online 15 October 2006; doi:10.1038/ng1903

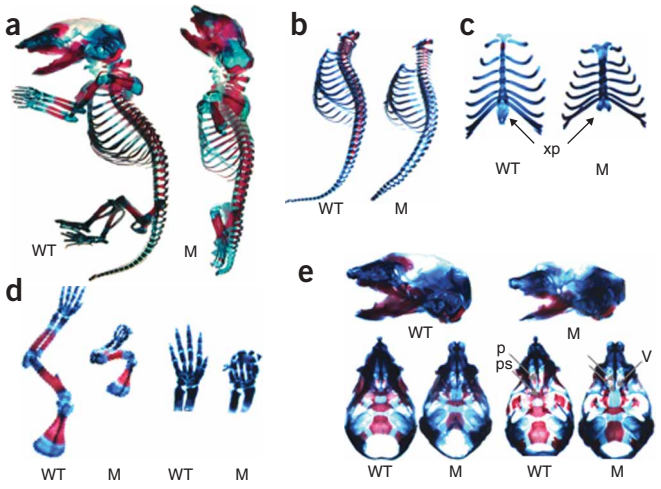

Figure 2 Skeletal defects in mice deficient for *Irf6*. (**a**) Skeletal structures of E17.5 wild-type (WT) and newborn mutant (M) embryos were stained for bone (alizarin red S) and cartilage (alcian blue). (**b**) The spine showed equal numbers of vertebrae in wild-type and null embryos. However, vertebrae in the mutant appeared smaller and showed delayed ossification. The mutant tail was substantially shorter. (**c**) There were equal numbers of ribs in the wild-type and null embryos, but the sternum appeared shorter with delayed ossification. The xiphoid process (xp) was bifid in the null embryo, demonstrating a failure of complete fusion of the thoracic cage. (**d**) The long bones were slightly shorter in null versus wild-type littermates, but both null and wild-type embryos showed normal surrounding muscle when skin was dissected. Proximal bones of the upper and lower limb were present in the null embryos, but distal structures, notably the digits, were severely abnormal. Forepaws were magnified to display synostosis of digits and absence of distal phalanges. (**e**) Skulls from wild-type and null embryos in lateral (top), superior (bottom left) and inferior (bottom right) views. Mandibles were removed for inferior views. The mandible in the null embryo was smaller with a narrower angle than in the wild-type, and the snout was also shorter in the null embryo. The palate shelves (p) in the wild-type embryo fuse along the midline, but the null embryo has a cleft palate. The palate shelves of null embryo are posteriorly and laterally displaced, allowing for direct viewing of nasal structures, including the vomer (v). The presphenoid (ps) is absent in the mutant. Similar results were obtained from three skeletal preparations.

Skeletal preparations showed that all four limbs and a tail had formed in the null embryos (**Fig. 2a**). However, the skeletal analysis showed abnormal vertebrae, tail (**Fig. 2b**), sternum, xiphoid process (**Fig. 2c**), digits (**Fig. 2d**) and skull, and there was a cleft of the secondary palate in the null embryos (**Fig. 2e**). The skeletal abnormalities are unexpected, as *Irf6* expression was not detected in developing bone (data not shown). However, similar skeletal abnormalities were observed in mice deficient for *Chuk* (also known as *Ikka*)[19]. *Chuk*, too, is not expressed in developing bone, and epidermal *Chuk* expression is sufficient to rescue the skeletal phenotype[20]. As in the case of *Chuk*-deficient mice, we speculate that the skeletal abnormalities in the *Irf6*-null mice are secondary to defects in epidermal differentiation (see below).

Histological analysis of skin showed wrinkles in epidermis from embryonic day (E) 17.5 wild-type embryos (**Fig. 3a**) but not in epidermis from null embryos (**Fig. 3b**). In wild-type embryos, the four stratified layers of the epidermis (basal, spinous, granular and cornified) were all present and visible. In the epidermis from null embryos, the basal layer was present along with a greatly expanded spinous layer, but the outer two layers appeared absent. Electron microscopy analysis of wild-type skin confirmed the presence of the electron-dense keratohyalin granules and the cornified outer layer (**Fig. 3c**). The epidermis from null embryos lacked these landmarks (**Fig. 3d**). The cornified layer serves as a barrier whose function can be measured qualitatively with toluidine blue, a dye that does not penetrate mature skin. We observed that toluidine blue was excluded from the epidermis of E17.5 wild-type embryos but not from the epidermis of null embryos (**Fig. 3e,f**).

To determine whether the expanded spinous layer resulted from increased cell proliferation and/or decreased programmed cell death, we performed BrdU and TdT-mediated dUTP nick end labeling (TUNEL) analyses, respectively. The epidermis from E17.5 wild-type embryos incorporated BrdU in the basal layer but not in the suprabasal layers (**Fig. 3g**). However, the epidermis obtained from null embryos incorporated BrdU in the basal and spinous layers (**Fig. 3h**). We also observed TUNEL staining in the epidermis from wild-type embryos but not from null embryos (**Fig. 3i,j**). Thus, proliferation in the spinous layer and a failure of keratinocytes to terminally differentiate contribute to an increase in the thickness of the spinous layer in mice deficient for *Irf6*.

We performed microarray and immunostaining analyses to characterize the molecular changes in skin from *Irf6* null embryos. We observed significant changes in the level of expression ($\geq$1.8-fold with $P \leq 0.05$) for 573 genes, including 42 of 80 protein markers for epidermal differentiation (**Table 1** and **Supplementary Table 1** online). The expression levels of 21 of 28 markers, including loricrin (**Fig. 3k,l**) and filaggrin (**Fig. 3m,n**), decreased significantly in the granular and cornified layers. In the expanded spinous layer, we observed no change or an increase in gene expression for all markers ($n = 25$), including keratin 1 (K1) (**Fig. 3o,p**). However, Irf6 was greatly decreased owing to the gene trap mutation (**Fig. 3q,r**). Notably, we also observed changes in expression for markers of the basal layer (**Table 1**). Keratin 14 (K14) and p63 were expressed ectopically in the spinous layer of the epidermis from null embryos (**Fig. 3s–v**). Thus, mice that are deficient for *Irf6* do not silence K14 and p63 in the spinous layer. In total, based on the abnormal epidermal histology, barrier function, cell proliferation, cell death and gene expression, we conclude that *Irf6* is necessary for regulating proliferation and terminal differentiation of keratinocytes.

Rac1, a Rho guanosine triphosphatase, is expressed primarily in the basal layer of the epidermis and regulates proliferation and differentiation by maintaining the stem cell compartment[21]. To test for a possible relationship between *Irf6* and *Rac1*, we compared the expression of *Rac1* in skin from wild-type and null E17.5 embryos. From the microarray analysis, we did not observe significant quantitative changes in expression of *Rac1* (**Table 1**). Also, we did not detect qualitative changes in expression of Rac1 using immunostaining (data not shown). These results suggest that *Rac1* is epistatic to *Irf6* in regulating keratinocyte differentiation or that they operate in independent pathways.

In the *Irf6*-null embryos, we observed epidermal adhesions at several sites, including the oral cavity (**Fig. 4a,b**), between the tail and hindlimbs (**Fig. 4c,d**) and in the esophagus (**Fig. 4e,f**). In contrast, we observed an oral adhesion in only 2 of 18 heterozygous embryos. The oral adhesions were unilateral and located superficial to the developing first or second molar (**Fig. 4g**). A similar phenotype was recently observed[22] in mice heterozygous for the R84C variant in *Irf6*. The R84C variant is highly associated with popliteal pterygium syndrome[8]. In a paper published in this issue[22], the authors observed oral adhesions in 89% (25 of 28) of heterozygous embryos, and all adhesions were bilateral. Moreover, they observed epidermal adhesions between the ventral surface of the tongue and the floor of the mouth.

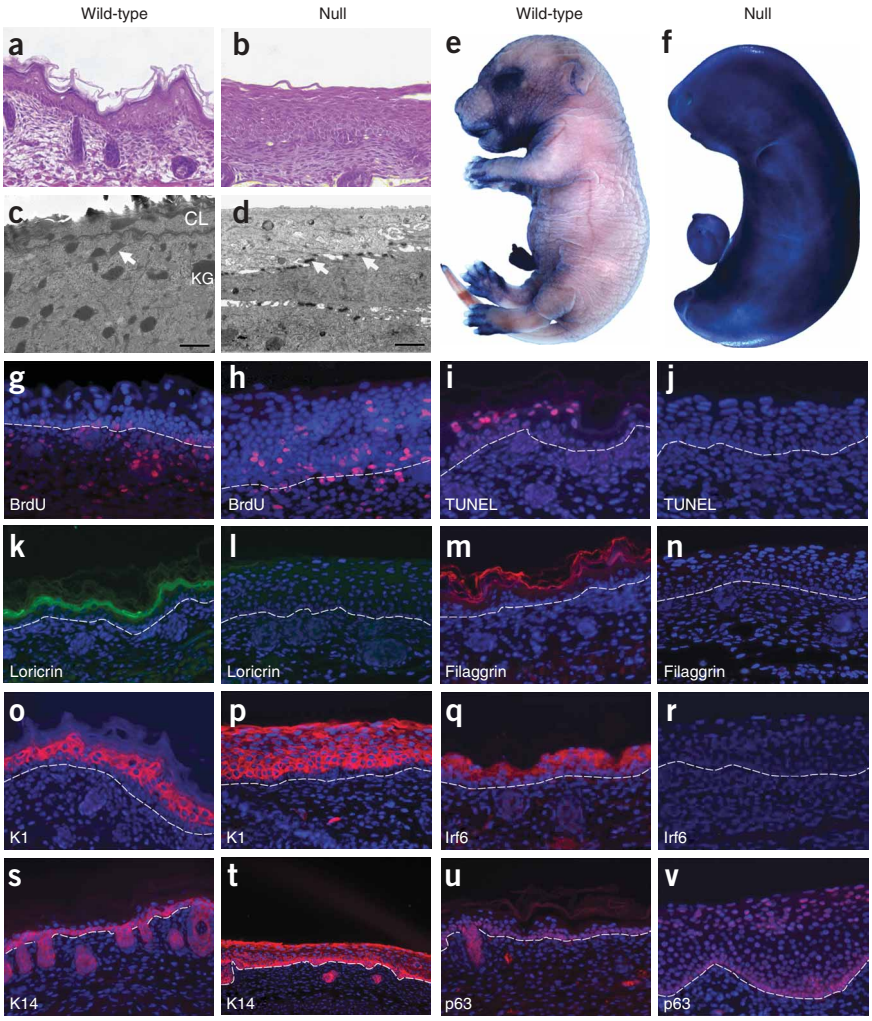

Figure 3 Histologic and molecular analyses of *Irf6*-null E17.5 embryos. (**a**–**d**) Hematoxylin and eosin–stained sections (**a**,**b**) and electron micrographs (**c**,**d**) of back skin. Note the presence of keratohyalin granules (KG) in the granular layer and a cornified layer (CL) of wild-type epidermis (**c**), which are absent in null epidermis (**d**). Arrows indicate desmosomes. Dye exclusion assays of whole embryos show a functional barrier in wild-type (**e**) but not in null (**f**) embryos. Cellular proliferation and programmed cell death were evaluated by BrdU (**g**,**h**) and TUNEL (**i**,**j**) staining, respectively. Immunofluorescent staining (red, except loricrin is green) for cornified and granular layers (**k**–**m**) and for spinous (**o**–**r**) and basal (**s**–**v**) layers. Proteins against which antibodies were directed are indicated. Nuclei were counterstained with DAPI (blue), and the basement membrane is indicated by the dashed line.

We did not observe adhesions in this location in embryos heterozygous for the gene trap allele. Both *Irf6* mutant strains were on a similar mixed genetic background of C57Bl/6 and 129/SvJ, suggesting that the phenotypic changes were due to allele differences.

To further characterize the epidermal adhesions observed in the null embryos, we performed electron microscopy and immunostaining analyses. We detected desmosomes, an important structure in the junctional complex between epithelial cells, in the epidermis of both wild-type and null E17.5 embryos (**Fig. 4h**,**i**). However, desmosomes in the epidermis of wild-type embryos were not observed in the most superficial layer, whereas desmosomes in the epidermis of null embryos were observed throughout the epidermis, including the most superficial regions (**Fig. 3c**,**d**). Microarray analysis (**Table 1**) showed that the expression of the desmosomal components either increased or did not change significantly. In addition, the subcellular localization of the desmocollin proteins did not seem to differ between wild-type and null epidermis (**Fig. 4j**,**k**). We speculate that the epidermal adhesions observed in the *Irf6*-null embryos result from the absence of the normal cornified layer. Without the cornified layer, cell interactions, including desmosomes, can occur between cells from adjoining tissues.

The morphological, skeletal and histological abnormalities in *Irf6*-null embryos are very similar to the phenotypes observed in the repeated epilation (*Er*) mouse[23] and mice that are deficient for the IkB kinase 1 gene (*Chuk*, also known as *Ikka*)[19]. Recently, two groups demonstrated that the *Er* phenotype results from a frameshift mutation in stratifin (*Sfn*)[24,25], a member of the 14-3-3 protein family. Two possible mechanisms for the common phenotype are that *Irf6* is necessary for the expression of *Chuk* and *Sfn* in skin or that Irf6 protein interacts with Ikka and Sfn. The microarray analysis did not show any significant change in the expression level of *Chuk* in the skin from E17.5 null embryos and showed a 3.3-fold increase in the expression level of *Sfn* (**Table 1**). Protein blot analysis confirmed these results (**Fig. 5a**,**b**). Immunostaining showed that Sfn (**Fig. 5c**,**d**) and Ikka (**Fig. 5e**,**f**) were expressed in the spinous layer of wild-type embryos, with some Ikka expression in the basal layer. No change occurred in the epidermis of the null embryos. To test for a direct protein interaction between Irf6 and Ikka or Sfn, we performed coimmunoprecipitation. Antibodies specific for each of these proteins did not pull down either of the other two proteins, but the antibody for Ikka readily pulled down Ikkb, another member of the Ikk complex (data not shown). We conclude that *Irf6* is not necessary for the expression of *Chuk* and *Sfn* in epidermis, that Irf6 does not form a detectable complex with Ikka and Sfn in epidermis and that other mechanisms are responsible for the common phenotype observed in mouse strains with mutations in each of these genes.

We report here that mice deficient for *Irf6* have abnormal skin, limb and craniofacial morphogenesis. The major histological feature of the *Irf6*-null mice is the lack of a normal stratified epidermis. The null epidermis was thicker than in wild-type mice, and the suprabasal keratinocytes failed to stop proliferating and failed to terminally differentiate. We conclude that a significant role for *Irf6* is to regulate proliferation and differentiation of keratinocytes.

In humans, mutations in *IRF6* cause two related orofacial clefting disorders, Van der Woude (VWS) and popliteal ptyergium syndromes (PPS)[8]. Both VWS and PPS show an autosomal dominant pattern of inheritance, whereas mice heterozygous for the *Irf6* null allele display a low-penetrance oral adhesion phenotype rather than a highly penetrant orofacial cleft phenotype. Although mice homozygous for the null *Irf6* allele have a cleft palate, the cleft seems to be caused by a defect in elevation, which could occur as a primary defect or could be

Table 1 Change in gene expression for markers representative of epidermal differentiation in skin from wild-type versus *Irf6*-null E17.5 embryos

Gene	Accession number	Layer	Change in expression (as a multiple of WT control)	Chromosome
Small proline rich–like family	AK003705	G,C	–310.8	3F1
Loricrin	NM_008508	G,C	–7.3	3F1
Filaggrin	J03458	G,C	–2.6	3F2
Desmocollin 1	NM_013504	S,G	NS	18
Small proline-rich 2a	NM_011468	S,G	16.9	3F1
Keratin 2-6b	NM_010669	S(i)	156.1	15F2
Irf6	NM_016851	S	–20.4	1H6
Stratifin	NM_018754	S	3.3	4D3
Desmocollin 2	NM_013505	S	8.1	18
Keratin 2-1	NM_008473	S	NS	15
Keratin 1-10	AK014360	S	NS	11
S100a8	NM_013650	B,S(i)	61.8	3F1
S100a9	NM_009114	B,S(i)	85.1	3F1
IkB kinase 1	NM_007700	B,S	NS	19
Rac1	BC003828	B	NS	5
p63	AF075436	B	1.7	16
Keratin 1-14	BC011074	B	2.4	11
Desmocollin 3	BB006344	B	2.9	18

Epidermal layers in which each gene is expressed in wild-type embryo are basal (B), spinous (S), granular (G) and cornified (C). Expression in a layer may be inducible (i), increase (positive), decrease (negative) or not change significantly (NS). WT, wild-type.

secondary to crowding of the craniofacial structures owing to the constrictive action of the skin or oral adhesions.

In addition to the oral facial clefts, individuals with PPS may present with a combination of eyelid adhesions (ankyloblepharon), oral adhesions, syndactyly of digits and pterygia[11]. Previously, we proposed that the additional abnormalities seen in individuals with PPS are due to a dominant-negative effect of the R84C variant[8]. The phenotypes of the *Irf6* mutant mice described here and in the accompanying report[22] are consistent with this model. First, the skin phenotypes in the mice homozygous for both *Irf6* alleles resemble the pterygia seen in individuals with PPS, with the much more severe phenotype in mice representing the null condition. Second, the phenotype observed in mouse embryos heterozygous for the R84C variant has a higher penetrance (89% versus 11%) and is more severe (multiple versus single sites) than the phenotype observed in mouse embryos heterozygous for the null allele. We recognize that this genotype-phenotype relationship for *Irf6* mutations is not absolute in either humans or mice. Thus, other factors contribute to the *IRF6* spectrum of phenotypes.

The earliest phenotype observed in the skin of *Irf6*-null mice was ectopic K14 expression in the spinous layer, suggesting a role for Irf6 in repressing K14 transcription. A previous study showed that two other transcription factors expressed in the spinous layer, Skin-1a and Tst-1, contribute to the repression of K14 (ref. 26). Also, Skin-1a bound directly to CREB-binding protein (CBP), suggesting that repression of the K14 promoter may be due to interference of the CBP/p300 coactivator

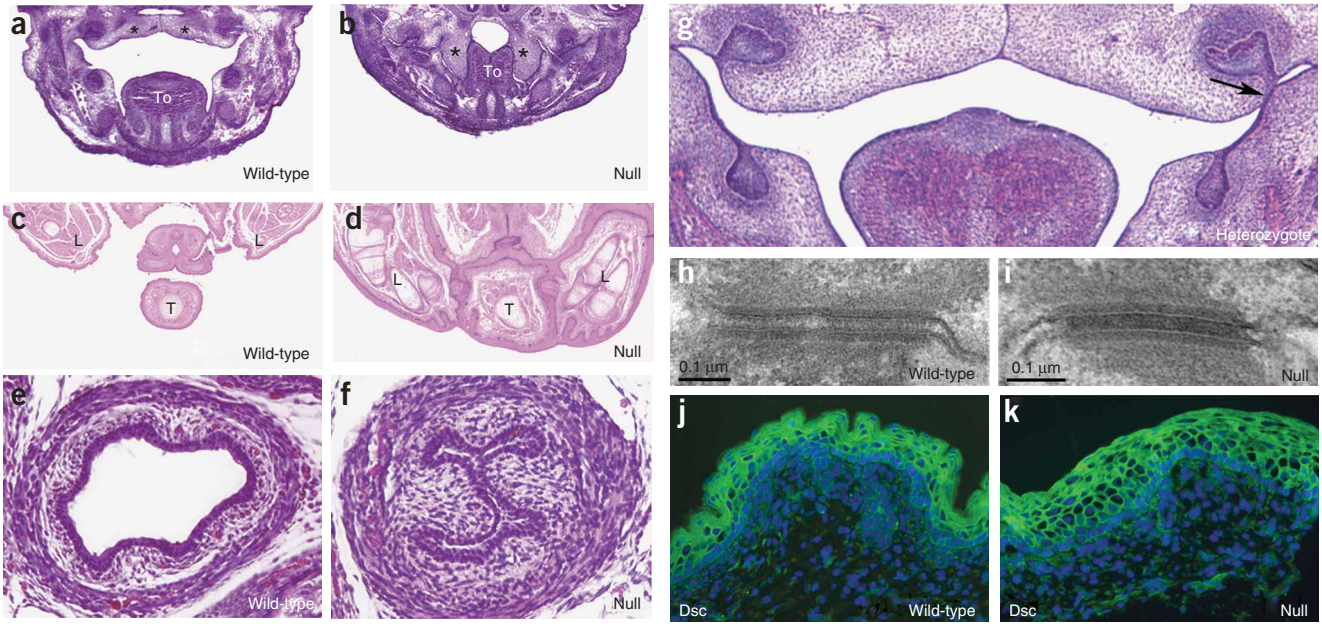

Figure 4 Epidermal adhesions and desmosomal structure in *Irf6*-null embryos. (**a**–**f**) Hematoxylin and eosin staining for sections of E14.5 frontal head (**a**,**b**), E17.5 rostral trunk (**c**,**d**) and E17.5 caudal trunk (**e**,**f**). Palate shelves elevate and begin to fuse in wild-type mice (**a**) but not in null embryos (**b**), where adhesions contribute to crowding of the oral cavity and prevent the palate shelves from elevating. Hindlimbs and tail are joined by epithelial adhesions (compare **c** with **d**). Esophagus is closed in null embryo (compare **e** with **f**). *: palate shelves; To: tongue; L: hindlimb; T: tail. Adhesion in the heterozygote was observed superficial to the first molar on the left side only (**g**, arrow). (**h**,**i**) Electron micrographs of desmosomes. Immunofluorescent staining (green) for desmocollin (Dsc) (**j**,**k**). We did not observe any difference in desmosomal structure and protein between wild-type and null embryos. Nuclei were counterstained with DAPI (blue).

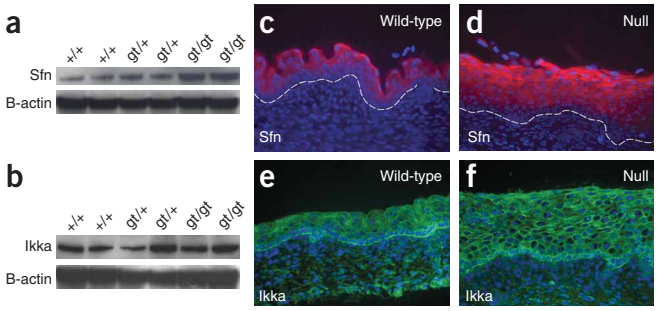

Figure 5 Expression of stratifin and Ikka in skin from *Irf6*-null E17.5 embryos. (**a**,**b**) Protein blot analyses show that stratifin expression (**a**) is greater in null embryos, whereas Ikka expression (**b**) does not seem to change. The respective blots were stripped and reprobed with β-actin as a control for loading. (**c**) Immunostaining shows that stratifin is expressed in the cytoplasm of spinous cells in skin from wild-type E17.5 embryos (**c**); it remains cytoplasmic but increases along with the expanded spinous layer in the skin from null embryos (**d**). (**e**,**f**) Immunostaining shows that Ikka is expressed predominantly in the basal layer in skin from both the wild-type (**e**) and *Irf6*-null (**f**) embryos. Ikka is localized to the cytoplasm and in the nucleus of some cells. This distribution does not appear to differ in skin from wild-type and *Irf6*-null embryos.

complex. Because IRF1 (ref. 27), IRF3 (ref. 28) and IRF7 (ref. 29) interact with CBP and/or p300, it is possible that IRF6 interacts with the CBP/p300 coactivator complex to help repress K14 expression in the spinous layer and to regulate other events in keratinocyte differentiation such as cessation of cell proliferation[30]. These new roles for a member of the IRF family expand the repertoire of IRF functions from stress response into development but suggest a bridge that spans these apparently disparate functions.

METHODS

Generation of mice deficient for *Irf6*. We obtained the embryonic stem (ES) cell line OST398253 that contains the gene trap allele for *Irf6* from Lexicon Genetics. The ES cells were microinjected into C57BL/6 blastocysts, and we obtained five male chimeras that were mated with C57BL/6 mice. Offspring with agouti coat color were genotyped for germline transmission of the gene trap allele. Maintenance and handling of mice were approved by the Animal Care Unit at the University of Iowa.

Genotyping of mutant mice. We used a PCR-based assay to genotype the gene trap cell line and subsequent mutant mice. Genomic DNA was isolated as recommended (Model 850 Alpha, Autogen) from mouse tail clips or embryonic tissues. PCR primers a and b flank the insertion site and detect the wild-type allele by amplifying a 461-bp product. Primer v, derived from the long terminal repeat of the vector, and primer b detect the gene trap allele by amplifying a 283-bp product. Primer sequences are listed in **Supplementary Table 2** online.

Protein blot analysis. Protein was purified as recommended (PARIS, Ambion) and quantified with a bicinchoninic acid (BCA) assay (Sigma). Total protein was separated in a 10% denaturing polyacrylamide gel (Invitrogen). We used 10, 20 and 50 μg of protein from skin per lane to detect Irf6, Sfn and Ikka, respectively. Transfer to a nylon membrane was performed as recommended (Invitrogen). We generated rabbit polyclonal antibodies against Irf6 (ref. 17) and purchased antibodies for Sfn and Ikka (Santa Cruz Biotech). The primary antibodies were detected as recommended using the ECL Plus kit (Amersham Biosciences). The blots were stripped and reprobed with a monoclonal antibody to β-actin. Blots were exposed to film for ≤1 min to detect β-actin, Irf6 and stratifin and were exposed for 15 min to detect Ikka.

Morphological analysis of mice. Null embryos were obtained from $Irf6^{+/gt1}$ matings. The presence of a copulation plug was defined as E0.5. Embryos were removed from euthanized mothers, analyzed and genotyped as above. Examination of skeletal morphology was done at E17.5. The skin was removed from wild-type and null embryos; it was then fixed in 40% formaldehyde/glacial acetic acid/70% ethanol mix (1:1:8 ratio), rinsed and then stained with alcian blue 8GX and alizarin red S (Sigma) to stain cartilage and calcified bone, respectively.

Histological analysis of mouse tissue. Embryos were fixed overnight in freshly prepared 4% paraformaldehyde and paraffin processed using standard methods. Sections (5 μm) were deparaffinized and stained with hematoxylin and eosin (SurgiPath) to visualize structures.

***In vivo* barrier assay.** The *in vivo* epidermal barrier assay was performed on E17.5 embryos using a dye exclusion assay. Embryos were fixed in 100% methanol for 5 min, rinsed briefly with PBS, stained in 0.1% toluidine blue for 1 min and washed several times with PBS.

Immunohistological analysis of mouse skin. Immunostaining was performed by incubating deparaffinized or unfixed frozen sections with antibodies at 4 °C overnight. Polyclonal antibodies were detected with Alexa 568–conjugated (Invitrogen) or FITC-conjugated (Jackson Immuno Research Laboratories) goat anti-rabbit secondary antibody as recommended. Monoclonal antibodies were detected either with the MOM kit (Vector Laboratories) followed by Strep-Alexa 568 (Invitrogen) or directly with a fluorescein isothiocyanate (FITC)-conjugated anti-loricrin (Covance). Slides were rinsed and mounted with Vectashield with 4,6-diamidino-2-phenylindole (DAPI) (Vector Laboratories) for visualization of nuclei. Antibodies were purchased for K1 (Novocastra), K14 (Novocastra), filaggrin (Novocastra), Irf6 (ref. 17), Sfn (Santa Cruz Biotech), Ikka (Santa Cruz Biotech), Rac1 (Chemicon) and desmocollin (Abcam).

Transmission electron microscopy of mouse skin. Skin from wild-type and null animals was fixed in 2.5% glutaraldehyde in 0.1 M cacodylate buffer. Samples were washed and postfixed in 1% osmium and then embedded in Epon 12. Thin sections (70 nm) were counterstained with uranyl acetate and lead citrate before visualization.

BrdU assay. Pregnant mothers were injected with BrdU (Sigma) (100 μg per g pregnant dam weight) 2 h before killing. BrdU immunostaining was performed as above with a monoclonal antibody to BrdU (Dako).

TUNEL assay. The TUNEL assay (Trevigen) was performed as recommended. Slides were counterstained with DAPI to identify TUNEL-positive cells.

Microarray analysis. Total RNA was isolated from E17.5 skin. First, we observed that the average mass of skin was significantly higher for null mice (70 mg ± 20 mg (s.d.) for wild-type skin ($n = 3$) versus 150 mg ± 30 mg (s.d.) for null skin ($n = 3$); $P = 0.02$) and was consistent with the histological findings that skin obtained from null mice was thicker than skin obtained from wild-type littermates. Total RNA was isolated as recommended (RNeasy, Qiagen), except that tissue was treated with proteinase K (20 mg/ml) for 20 min at 55 °C. RNA was assessed for quality using the Model 2100 Bioanalyzer (Agilent Technologies). We processed 5 μg of total RNA for use on the microarray by using the Affymetrix GeneChip one-cycle target labeling kit (Affymetrix) according to the manufacturer's recommended protocols. The resultant biotinylated complementary RNA (cRNA) was fragmented and then hybridized to the GeneChip Mouse Genome 430 2.0 Array (Affymetrix). The arrays were washed, stained and scanned using the Affymetrix Model 450 Fluidics Station and Affymetrix Model 3000 Scanner by the University of Iowa DNA Core Facility using the manufacturer's recommended protocols. Expression values were generated using the Microarray Suite (MAS) v5.0 software (Affymetrix). CEL files were read into dChip, normalized and modeled using the perfect match-mismatch difference model. Negative values were truncated to a default value of 10. The 'present' and 'absent' calls used were those from MAS5. Excluding the Affymetrix control probes on the chip, a total of 30,250 probes were 'present'.

Statistical analysis. We defined genes that were expressed differentially as those showing at least a 1.8-fold difference between wild-type and mutant arrays. The

comparison parameters were as follows: 90% confidence bound for change in expression as a multiple of the control, $P \leq 0.05$ for testing whether wild-type expression was equal to mutant expression, and a paired t-test with $P \leq 0.05$. To compare the observed number of genotypes from heterozygous matings with the expected mendelian ratios, we used χ^2 analysis. To compare the mass of wild-type and mutant skin, we used Student's t-test.

Accession codes. Gene Expression Omnibus (GEO): microarray data, GSE5800.

Note: Supplementary information is available on the Nature Genetics website.

ACKNOWLEDGMENTS

The authors wish to acknowledge technical assistance from E. Sweezer, R. Cao, T. Kinney, S. Bullard, H. Mishima and A. Lidral. We also thank K. Walters and J. Shao of the Central Microscopy Research Facility and K. Knudtson of the DNA Core Facility at the University of Iowa. We wish to thank R. Richardson and M. Dixon for sharing results before publication. This work was supported in part by US National Institutes of Health grants DE16215 (J.C.M., B.C.S., M.L., B.Y.), DE13513 (B.C.S.) and DE08559 (J.C.M.).

AUTHOR CONTRIBUTIONS

This study was designed by B.C.S., S.K., J.C.M. and B.Y.; phenotype assessment was performed by C.R.I., A.K., K.J.T., M.D. and S.L.G.; genotype assessment was performed by M.I.M. and A.K.; data analysis was performed by S.S. and M.L.; and C.R.I., B.C.S., J.C.M., M.L., A.K. and M.D. contributed to the writing of the paper.

COMPETING INTERESTS STATEMENT

The authors declare that they have no competing financial interests.

Published online at http://www.nature.com/naturegenetics
Reprints and permissions information is available online at http://npg.nature.com/reprintsandpermissions/

1. Matsuyama, T. *et al.* Targeted disruption of IRF-1 or IRF-2 results in abnormal type I IFN gene induction and aberrant lymphocyte development. *Cell* **75**, 83–97 (1993).
2. Sato, M. *et al.* Distinct and essential roles of transcription factors IRF-3 and IRF-7 in response to viruses for IFN-alpha/beta gene induction. *Immunity* **13**, 539–548 (2000).
3. Mittrucker, H.W. *et al.* Requirement for the transcription factor LSIRF/IRF4 for mature B and T lymphocyte function. *Science* **275**, 540–543 (1997).
4. Takaoka, A. *et al.* Integral role of IRF-5 in the gene induction programme activated by Toll-like receptors. *Nature* **434**, 243–249 (2005).
5. Honda, K. *et al.* IRF-7 is the master regulator of type-I interferon-dependent immune responses. *Nature* **434**, 772–777 (2005).
6. Holtschke, T. *et al.* Immunodeficiency and chronic myelogenous leukemia-like syndrome in mice with a targeted mutation of the ICSBP gene. *Cell* **87**, 307–317 (1996).
7. Kimura, T. *et al.* Essential and non-redundant roles of p48 (ISGF3 gamma) and IRF-1 in both type I and type II interferon responses, as revealed by gene targeting studies. *Genes Cells* **1**, 115–124 (1996).
8. Kondo, S. *et al.* Mutations in *IRF6* cause Van der Woude and popliteal pterygium syndromes. *Nat. Genet.* **32**, 285–289 (2002).
9. Kayano, S. *et al.* Novel *IRF6* mutations in Japanese patients with Van der Woude syndrome: two missense mutations (R45Q and P396S) and a 17-kb deletion. *J. Hum. Genet.* **48**, 622–628 (2003).
10. Wang, X. *et al.* Novel mutations in the *IRF6* gene for Van der Woude syndrome. *Hum. Genet.* **113**, 382–386 (2003).
11. Zucchero, T.M. *et al.* Interferon regulatory factor 6 (*IRF6*) gene variants and the risk of isolated cleft lip or palate. *N. Engl. J. Med.* **351**, 769–780 (2004).
12. Blanton, S.H. *et al.* Variation in *IRF6* contributes to nonsyndromic cleft lip and palate. *Am. J. Med. Genet. A* **137**, 259–262 (2005).
13. Ghassibe, M. *et al.* Interferon regulatory factor-6: a gene predisposing to isolated cleft lip with or without cleft palate in the Belgian population. *Eur. J. Hum. Genet.* **13**, 1239–1242 (2005).
14. Scapoli, L. *et al.* Strong evidence of linkage disequilibrium between polymorphisms at the *IRF6* locus and nonsyndromic cleft lip with or without cleft palate, in an Italian population. *Am. J. Hum. Genet.* **76**, 180–183 (2005).
15. Srichomthong, C., Siriwan, P. & Shotelersuk, V. Significant association between *IRF6* 820G->A and non-syndromic cleft lip with or without cleft palate in the Thai population. *J. Med. Genet.* **42**, e46 (2005).
16. Zambrowicz, B.P. *et al.* Disruption and sequence identification of 2,000 genes in mouse embryonic stem cells. *Nature* **392**, 608–611 (1998).
17. Bailey, C.M. *et al.* Mammary serine protease inhibitor (Maspin) binds directly to interferon regulatory factor 6: identification of a novel serpin partnership. *J. Biol. Chem.* **280**, 34210–34217 (2005).
18. Knight, A.S., Schutte, B.C., Jiang, R. & Dixon, M.J. Developmental expression analysis of the mouse and chick orthologues of *IRF6*: the gene mutated in Van der Woude syndrome. *Dev. Dyn.* **235**, 1441–1447 (2006).
19. Hu, Y. *et al.* Abnormal morphogenesis but intact IKK activation in mice lacking the IKKalpha subunit of IkappaB kinase. *Science* **284**, 316–320 (1999).
20. Sil, A.K., Maeda, S., Sano, Y., Roop, D.R. & Karin, M. IkappaB kinase-alpha acts in the epidermis to control skeletal and craniofacial morphogenesis. *Nature* **428**, 660–664 (2004).
21. Benitah, S.A., Frye, M., Glogauer, M. & Watt, F.M. Stem cell depletion through epidermal deletion of Rac1. *Science* **309**, 933–935 (2005).
22. Richardson, R.J. *et al.* IRF6 is a key determinant of the keratinocyte proliferation-differentiation switch. *Nat. Genet.* advance online publication 15 October 2006 (doi:10.1038/ng1894).
23. Fisher, C., Jones, A. & Roop, D.R. Abnormal expression and processing of keratins in pupoid fetus (*pf/pf*) and repeated epilation (*Er/Er*) mutant mice. *J. Cell Biol.* **105**, 1807–1819 (1987).
24. Herron, B.J. *et al.* A mutation in stratifin is responsible for the repeated epilation (*Er*) phenotype in mice. *Nat. Genet.* **37**, 1210–1212 (2005).
25. Li, Q., Lu, Q., Estepa, G. & Verma, I.M. Identification of 14–3-3sigma mutation causing cutaneous abnormality in repeated-epilation mutant mouse. *Proc. Natl. Acad. Sci. USA* **102**, 15977–15982 (2005).
26. Sugihara, T.M., Kudryavtseva, E.I., Kumar, V., Horridge, J.J. & Andersen, B. The POU domain factor Skin-1a represses the keratin 14 promoter independent of DNA binding. A possible role for interactions between Skn-1a and CREB-binding protein/p300. *J. Biol. Chem.* **276**, 33036–33044 (2001).
27. Dornan, D. *et al.* Interferon regulatory factor 1 binding to p300 stimulates DNA-dependent acetylation of p53. *Mol. Cell. Biol.* **24**, 10083–10098 (2004).
28. Qin, B.Y. *et al.* Crystal structure of IRF-3 in complex with CBP. *Structure* **13**, 1269–1277 (2005).
29. Yang, H., Lin, C.H., Ma, G., Baffi, M.O. & Wathelet, M.G. Interferon regulatory factor-7 synergizes with other transcription factors through multiple interactions with p300/CBP coactivators. *J. Biol. Chem.* **278**, 15495–15504 (2003).
30. MacPartlin, M. *et al.* p300 regulates p63 transcriptional activity. *J. Biol. Chem.* **280**, 30604–30610 (2005).